

# Endoatmospheric Thrust Termination Condition to Achieve a Low Earth Orbit

Hideo Ikawa\*

Northrop Corporation, Pico Rivera, California 90660

During the launch of a winged spacecraft propelled by an air-breathing/rocket engine system into a prescribed orbit, the powered boost phase terminates and the unpowered orbit transfer phase begins in the atmosphere. The aerodynamic drag penalty by endoatmospheric coasting that depresses the orbit must be compensated at the time of the thrust termination. However, estimation of the future  $\Delta V$  penalty constitutes the highest uncertainty. The impact of this  $\Delta V$  penalty is equivalent to reaching a higher imaginary apogee that extends beyond the prescribed orbit. Therefore, an imaginary apogee trace is a useful indicator for assessing the endo-/exoatmospheric thrust termination effect. A supplemental event trapping procedure is derived that is based on the application of a simple idea but is powerful enough to offer an insight into the complex problem of endoatmospheric thrust termination to orbit. This technique can be added to the existing trajectory simulation programs to enhance their capability.

## Nomenclature

$C_D$	= drag coefficient
$e$	= eccentricity
$h$	= altitude, km
$I_{sp}$	= specific impulse, s
$K_D$	= inverse of ballistic coefficient, $C_D S_{ref}/2m$ , $m^2/kg$
$L/D$	= lift-to-drag ratio
$M_f$	= multiplying factor, Eq. (3)
$m$	= vehicle mass at burnout, kg
$R_a$	= prescribed apogee radius, km
$R_b$	= normalized apogee radius, $R_a/r > 1.0$
$r$	= local position radius, km
$S_{ref}$	= reference area, $m^2$
$T$	= thrust, N
$T/D$	= thrust-to-drag ratio
$t$	= time, s
$V$	= local velocity, km/s
$\beta$	= characteristic height for an exponential density, km
$\gamma$	= local flight-path angle, deg
$\Delta V$	= energy loss by aerodynamic and/or gravity, km/s
$\epsilon$	= bound for a convergence limit
$\rho$	= $\rho_0 e^{-h/\beta}$ , atmospheric density, $kg/m^3$
$\mu$	= universal gravitational constant, $m^3/s^2$

## Subscripts

$a$	= at apogee
$ae$	= aerodynamic drag
$bo$	= at burnout (thrust termination)
$ge$	= gravity
$i$	= inertial frame of reference
$o$	= at starting point
$r$	= relative frame of reference
$v$	= in vacuum

## Introduction

TO minimize the impact of aerodynamic drag loss on the ascent trajectory, conventional vertical launching methods are used for placing space vehicles into low Earth orbit. In

Presented as Paper 91-2901 at the AIAA Atmospheric Flight Mechanics Conference, New Orleans, LA, Aug. 12-14, 1991; received Sept. 13, 1991; revision received Jan. 23, 1992; accepted for publication Jan. 23, 1992. Copyright © 1991 by the American Institute of Aeronautics and Astronautics, Inc. All rights reserved.

\*Senior Technical Specialist, B-2 Division, Aerosciences Technology. Member AIAA.

this case a steep boost trajectory is programmed to escape rapidly from the endoatmospheric flight, identified as "all rocket" in Fig. 1. The vehicle is then commanded to follow a nearly horizontal, exoatmospheric acceleration path for acquiring the orbital transfer energy. The final unpowered orbit transfer is achieved essentially in vacuum. The advantage is that aerodynamic heating and energy losses associated with aerodynamic drag and gravity are minimized.

In recent years, however, technology development of a horizontal takeoff, single-stage-to-orbit aerospace plane concept has been revived (e.g., the National Aerospace Plane). A winged space vehicle propelled with an air-breathing/rocket engine propulsion system is of particular interest. Through this concept the powered boost trajectory follows a relatively high dynamic pressure corridor to achieve efficient air-breathing engine (AB) performance, shown as "winged AB/rocket" in Fig. 1. A relatively small angle-of-attack acceleration path is also maintained for achieving a fuel efficiency because the effective  $I_{sp}$  advantage of the supersonic combustion ramjet engine (SCRAMJET) diminishes rapidly with  $T/D$  reduction.<sup>1,2</sup> As a consequence, the powered boost terminates inevitably in atmosphere.

Unfortunately, in this case, a portion of the unpowered orbit transfer event also occurs in atmosphere between the thrust terminating altitude and the sensible edge of atmosphere. The energy loss produced by aerodynamic drag is therefore unavoidable during the coasting event, as observed

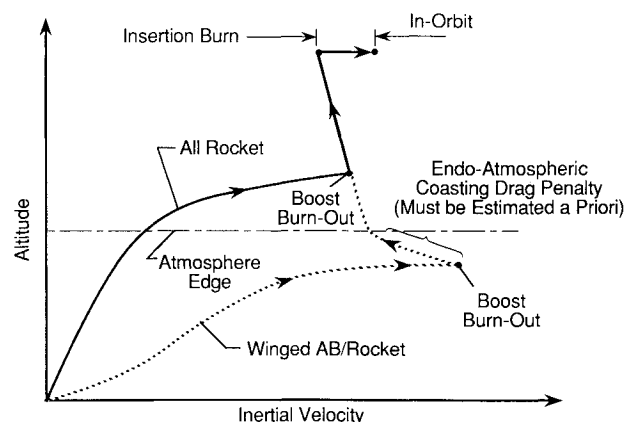


Fig. 1 Ascent trajectory comparison of all rockets and winged air-breathing/rocket engine vehicles.

in Fig. 1. This  $\Delta V$  penalty must be compensated at the time of the powered boost termination in order for the vehicle to be placed on a proper orbit. However, the expected aerodynamic drag is unknown a priori at the time of thrust termination. Because the  $\Delta V$  penalty is equivalent to reaching a higher imaginary apogee, the apogee trace is a useful tool for identifying the endo-/exoatmospheric thrust termination requirements.

The trajectory can be simulated by application of well-established methods such as the POST<sup>3</sup> and OTIS<sup>4</sup> programs. However, the endoatmospheric thrust termination portion of an orbital trajectory optimization is quite difficult because the engine and aerodynamic performances are sensitive to the vehicle maneuvers and atmospheric variation. For example, the users of POST may experience difficulty in defining a phase for establishing the required endoatmospheric burnout condition for a targeted orbit without having a first-hand knowledge of the nominal condition. To the best of the author's knowledge, a constant numerical value criterion of either a cutoff velocity, a depleted propellant, or an altitude must be specified for the phase termination of POST. However, the required cutoff velocity is not constant and continuously changes during the terminal phase of the power boost for both endo-/exoatmospheric thrust terminations.

A supplemental event trapping procedure based on the application of a simple idea but powerful enough to offer insight into the complex problem of endoatmospheric thrust termination to orbit is discussed here. In this approach the required cutoff velocity is continuously computed and monitored during the terminal phase of the power boost. The intention of this technique is not to replace the established trajectory simulation programs, but rather to improve the capability of these programs by introducing an simplified event trapping procedure. With this technique a novice engineering student is able to simulate a preliminary orbital trajectory of a winged spacecraft.

### Methodology

An event trapping procedure that identifies a required condition for an endoatmospheric thrust termination to place a winged spacecraft on a precisely targeted orbit is derived. This supplemental procedure can be incorporated into any existing trajectory simulation program, including POST and OTIS. The transfer energy requirement for thrust termination consists of a sum of the ideal inertial velocity to reach an apogee and the  $\Delta V$  penalty produced by an endoatmospheric coasting. It must be emphasized that the required cutoff velocity is continuously changing during the terminal phase of the power boost.

#### Ideal Inertial Velocity for Orbit Transfer

A transfer energy requirement for the powered-boost termination in vacuum to place a vehicle on a proper transfer ellipse is dictated by the law of Keplerian orbital mechanics.<sup>5,6</sup> For this analysis the targeted apogee radius is defined by the prescribed orbital radius. At each integration step during the boost trajectory simulation, a required local inertial velocity<sup>7</sup> for reaching a targeted apogee is predicted as a function of the local position radius and inertial flight-path angle as follows:

$$V_{iv} = (\mu Q/r)^{1/2} \quad (1)$$

where

$$Q(R_b, \gamma_i) = \frac{2R_b(R_b - 1)}{(R_b^2 - \cos^2 \gamma_i)} \quad (2)$$

#### Endoatmospheric Coasting $\Delta V$

When the powered boost is terminated and the unpowered coasting begins in atmosphere, the ideal transfer ellipse decays as the coasting aerodynamic drag dissipates the transfer energy. To achieve a proper orbit, this coasting  $\Delta V$  penalty must be compensated at the time of the powered-boost termination.

However, this  $\Delta V$  prediction constitutes the highest uncertainty in trajectory analysis because the future histories of Mach number, altitude, and vehicle attitude beyond the thrust termination are not clearly defined a priori during the powered boost. Therefore, a reasonable  $\Delta V$  loss of the subsequent coasting event, from an altitude on each integration step to the edge of the sensible atmosphere, must be pre-estimated and corrected during the powered boost.

For an exponential atmosphere a  $\Delta V$  penalty for an unpowered coasting event can be expressed as

$$\Delta V_r = V_{r1} \left[ 1.0 - \exp \left( \frac{M_f K_D}{\sin \gamma_r} \beta \Delta \rho \right) \right] \quad (3)$$

where  $\Delta \rho = \rho(h_2) - \rho(h_1) < 0$  and  $K_D$  is defined for a minimum  $C_D$  angle of attack.

$M_f$  is included to account for uncertainties in nominal values of drag coefficient and flight-path angle because both parameters may vary during the coasting event. For example, a constant  $K_D$  is assumed because a hypersonic Mach number freeze is normally an accepted phenomenon for a given flight attitude. In reality, however, the drag coefficient increases with respect to altitude by a hypersonic viscous interaction in low-density atmosphere (an altitude greater than  $\sim 60$  km) and changes with varying flight profile.

Similarly, a constant  $\gamma_r$  is also assumed because a shallow flight path is followed during the powered boost and is expected to vary slightly during the endoatmospheric coasting event. The flight-path angle, however, may vary proportionally with respect to  $L/D$ .

#### Thrust Termination Velocity

At each integration step, a required thrust termination velocity is estimated by summing a predicted inertial velocity in vacuum [Eq. (1)] and a coasting  $\Delta V_r$  penalty [Eq. (3)]. An imaginary apogee at the thrust termination is determined by this velocity:

$$V_{ibo} = V_{iv} + \Delta V_r \quad (4)$$

The local trajectory parameters are calculated by integrating the equations of motion (e.g., as given in Ref. 7). The parameters of interest are time, vehicle mass, local altitude (position radius), velocity, and flight-path angle. The resulting position radius and inertial flight-path angle are used to compute  $V_{iv}$ . The relative velocity, flight-path angle, and atmospheric density are used to estimate  $\Delta V_r$ .

#### Event Trapping Procedure

A flowchart for the event trapping iteration procedure is shown in Fig. 2. At each integration step taken from the referenced starting point [defined just prior to the burnout (BO)], the local trajectory parameters are computed and the required BO velocity is predicted. Then the integrated local inertial velocity and the predicted BO velocity are compared. When the integrated velocity is found to be smaller than the BO velocity,  $V_i < V_{ibo}$ , then the integration is advanced to next time step,  $t = t + \Delta t$ , until both velocities are matched.

At the matched point,  $|V_i - V_{ibo}| < \epsilon$ , a sufficient energy to reach the prescribed orbit is acquired and the peak imaginary apogee is established. At this point, the powered boost is terminated and the trajectory parameters for the thrust termination are defined.

The coasting phase from the BO point to the apogee follows next. However, the imaginary apogee of the transfer ellipse decays during the time the vehicle traverses through the atmosphere. The equations of motion for the coasting phase are integrated until the flight-path angle approaches zero at the apogee.

The next step is to compare the actually computed  $r_a$  with the prescribed  $R_a$  at the apogee. When the condition  $|R_a - r_a| < \epsilon_a$  is met, the solution has converged. If  $|R_a - r_a| > \epsilon_a$ , the

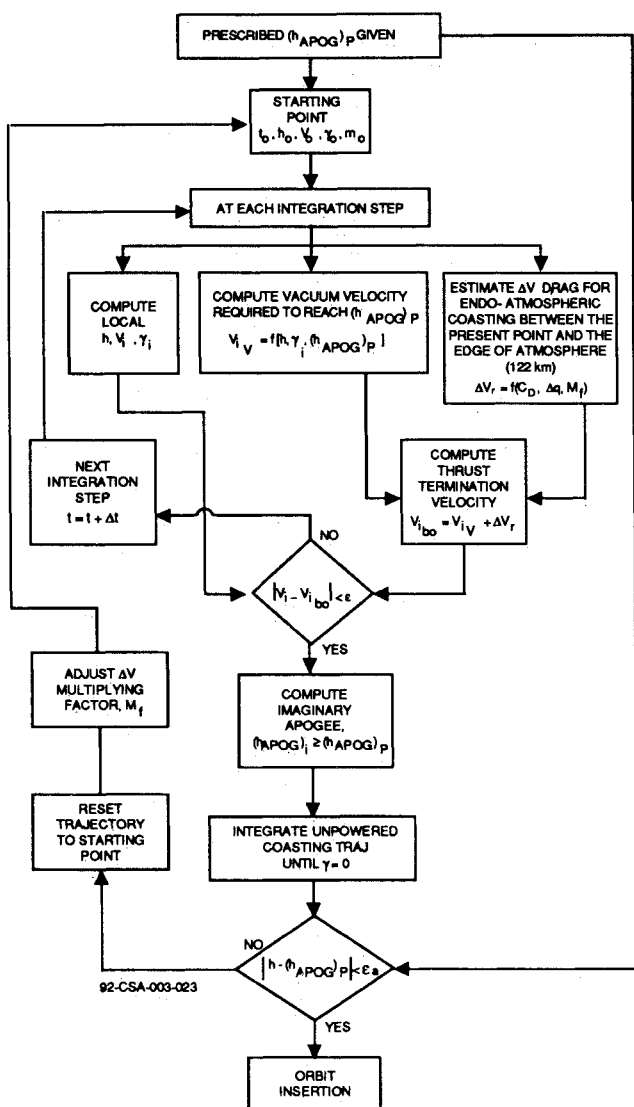


Fig. 2 Flowchart for determining an endoatmospheric thrust termination for placing a winged spacecraft into a prescribed orbit.

computational process will be reset to the referenced starting point. The  $M_f$  will be adjusted and the iteration is repeated until both apogee altitudes have converged.

Note that the aerodynamic contribution is based on the relative velocity, whereas the required BO velocity to orbit is defined in terms of the inertial velocity. For flights over the rotational Earth, therefore, the present computational process considers the orientation of the orbital inclination and latitude positions.

#### Application

The foregoing event trapping procedure can be inserted as a supplemental phase in any trajectory simulation program, including POST. For the present methodology validation the procedure was incorporated in a point mass, three-dimensional trajectory simulation program.<sup>8</sup> Each of the following sample problems was solved on a 386SX/16 based computer with a numerical processor in ~ 5 min.

#### Discussion of Results

##### Endoatmospheric Thrust Termination Trajectory

A sample trajectory for placing a winged spacecraft into a low Earth orbit was simulated. For demonstrating only the primary effect of endoatmospheric thrust termination, the boost phase trajectory established by the AB propulsion sys-

tem was not included. Without loss of generality, the rocket engines were used during the final boost stage to attain the orbital energy. Therefore, the reference starting conditions for iteration were arbitrarily established in the upper atmosphere: an altitude of 60.96 km (200 kft), an inertial velocity of 7.32 km/s (24 kft/s), and an inertial flight-path angle of 0.836 deg at the latitude position of 28 deg on a 30-deg inclined orbit. A 280.4-km (920 kft) orbital altitude was prescribed. A zero angle of attack was flown during the coasting phase.

Overall histories of the trajectory parameters are shown in Figs. 3-5, and the expanded views near the endo-/exoatmospheric flight transitions are shown in Figs. 6-9. Note that all line data represent the simulated trajectory parameters and the data points indicate the points where the event changes were executed.

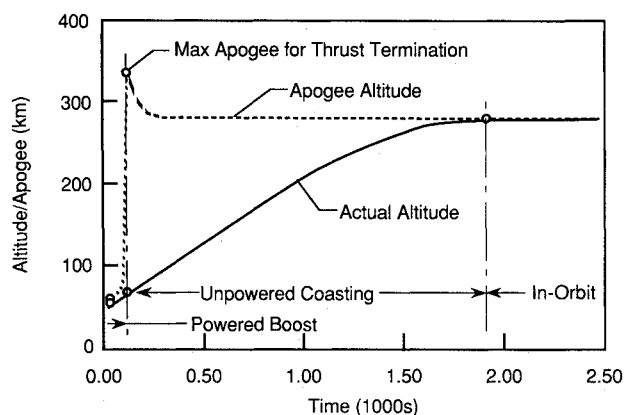


Fig. 3 Apogee/actual altitude histories to orbit ( $H_0 = 61$  km,  $V_{i0} = 7.332$  km/s, endoatmospheric thrust termination).

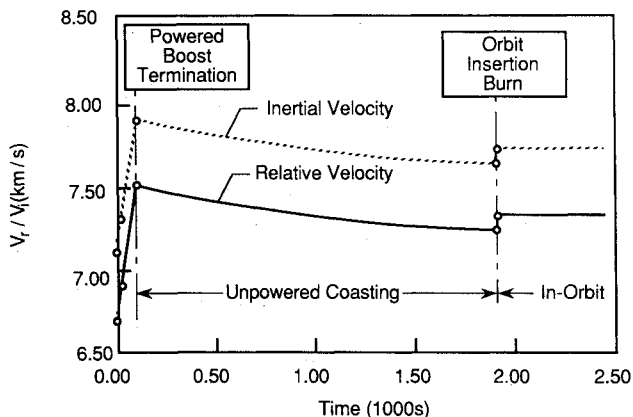


Fig. 4 Velocity histories to orbit, endoatmospheric thrust termination.

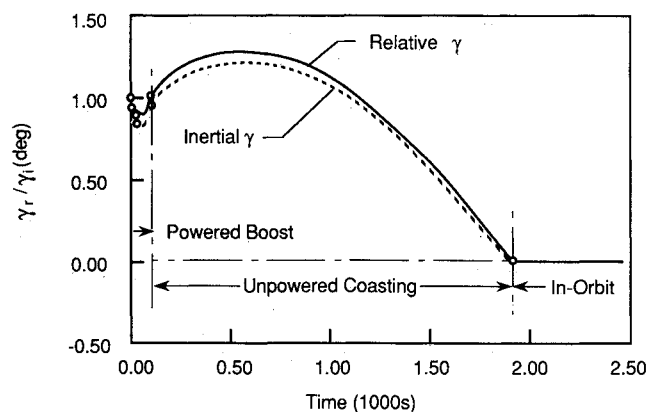


Fig. 5 Flight-path angle histories, endoatmospheric thrust termination.

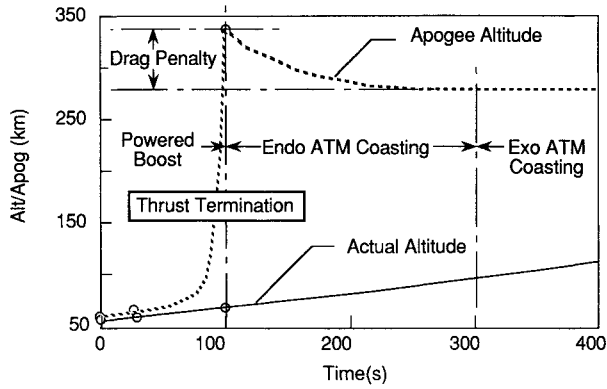


Fig. 6 Apogee/actual altitude histories near the endoatmospheric thrust termination.

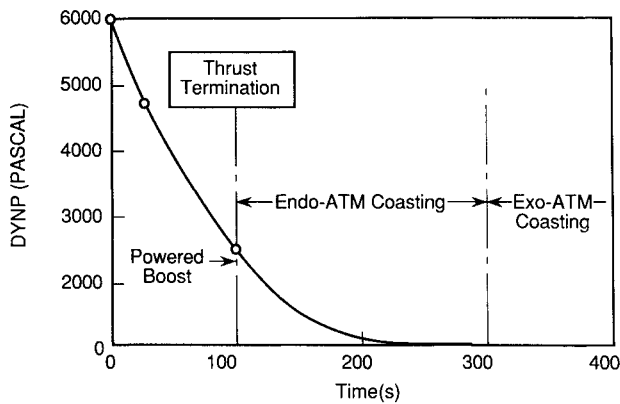


Fig. 7 Dynamic pressure history near the endoatmospheric thrust termination.

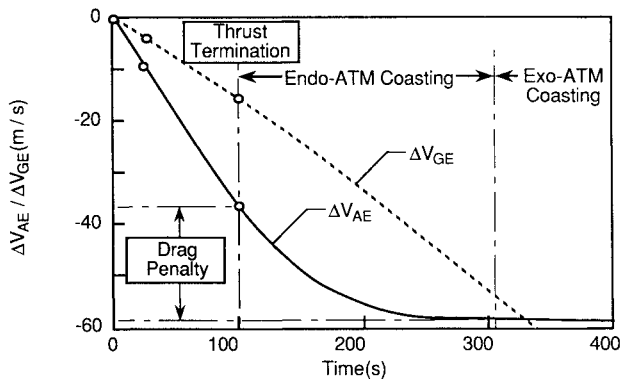


Fig. 8  $\Delta V$  histories near the endoatmospheric thrust termination.

The apogee and actual altitude histories from the iteration starting point to orbit are compared in Fig. 3. Toward the end of powered boost, the imaginary apogee altitude began to climb rapidly to establish the peak value at the time of the thrust termination. During the coasting phase below a 100-km altitude, the apogee decayed as the transfer energy was dissipated by aerodynamic drag. The exoatmospheric unpowered climb was indicated by the constant apogee trace achieved on the prescribed orbital altitude.

The inertial and the relative velocity histories are compared in Fig. 4. Because the impact of a  $\Delta V$  penalty induced by aerodynamic drag did not appear dramatically during the endoatmospheric coasting, the apogee trace is a better indicator for identifying the endo-/exoatmospheric flight. A very shallow flight path of  $<1.3$  deg was flown as shown in Fig. 5.

The expanded view (Fig. 6) delineates the decaying characteristics of apogee by the endoatmospheric coasting, which

had lasted almost 200 s. The additional energy requirement for the apogee overshoot of  $\sim 55$  km ( $\sim 20\%$  of the prescribed orbital altitude) was the penalty imposed by the endoatmospheric coasting.

The time the sensible edge of the atmosphere was reached can be easily defined by the dynamic pressure history at a point where the zero value is approached (Fig. 7) and by the  $\Delta V_{ae}$  history to where a constant value is approached (Fig. 8). A value of  $\Delta V_{ae} \approx 22$  m/s has penalized an apogee altitude by  $\sim 55$  km. The effect of aerodynamic drag to influence eccentricity of the transfer ellipse is delineated in Fig. 9. The eccentricity change of  $\sim 0.0025$ , which is normally considered as negligibly small, will impact the final outcome of satisfying the proper orbit requirement.

#### Synergetic Orbital Plane Change Simulation

A synergetic orbital plane change by a winged spacecraft requires endoatmospheric flight maneuvers. The initial in-orbit conditions were continued from the final orbit conditions

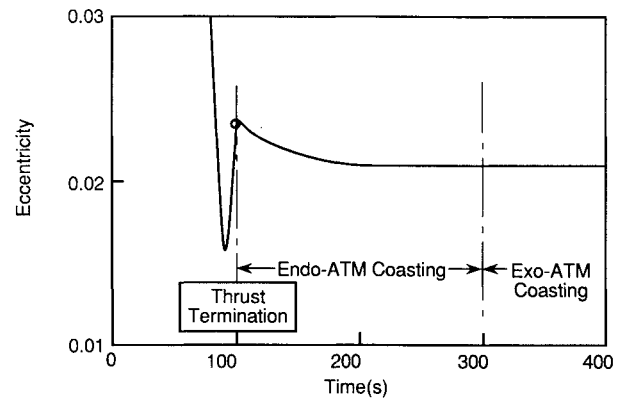


Fig. 9 Eccentricity history near the endoatmospheric thrust termination.

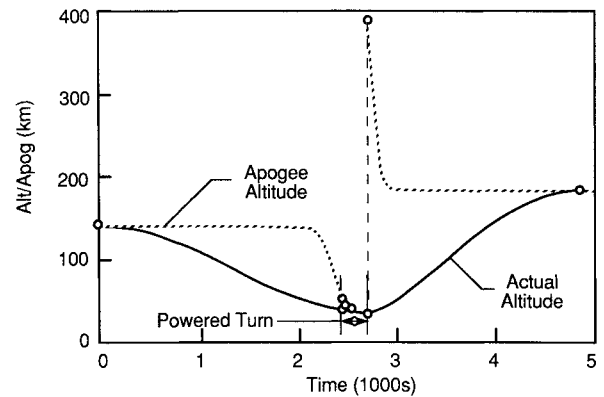


Fig. 10 Apogee/actual altitude histories, synergetic orbital change.

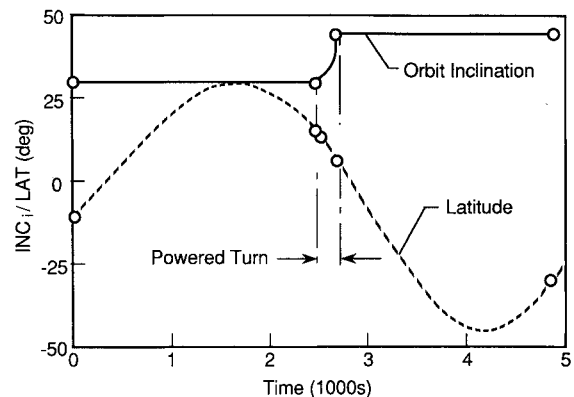


Fig. 11 Orbital inclination/latitude histories, synergetic orbital change.

of the previous sample case (see Figs. 3–5). The de-orbit burn was targeted in the upper atmosphere altitude of 70 km. An orbital plane change from the initial inclination of 30 deg to the final inclination of 45 deg was performed by the powered cruising turn in atmosphere. A new re-orbit altitude of 365.8 km was selected to demonstrate the versatility of the method.

The exoatmospheric orbit transfers were signified by the constant apogee traces as shown in Fig. 10. During the de-orbit phase the point of entry and descent in atmosphere were identified by the rapid decaying characteristic of the apogee trace. During the re-orbit phase a required thrust termination condition was properly captured and an apogee overshoot of almost twice the targeted orbital altitude was identified. A magnitude of the overshoot was substantially greater than the previous case (Fig. 3) because the flight-path angle at the endoatmospheric BO was smaller. An orbital inclination change of 15 deg and the resulting latitude traverse history are shown in Fig. 11.

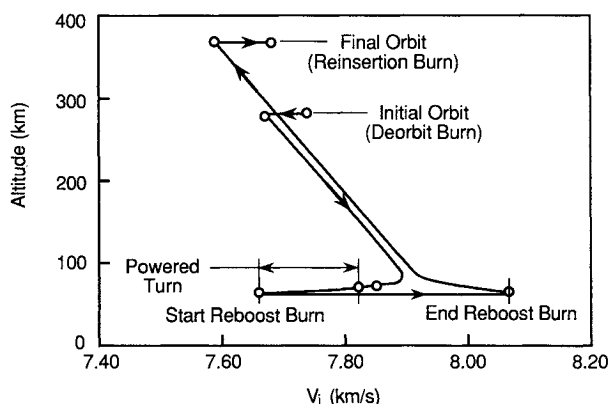


Fig. 12 Altitude vs inertial velocity, synergetic orbital change.

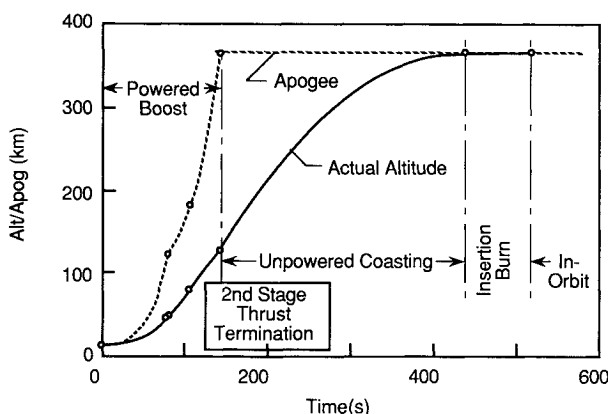


Fig. 13 Apogee/actual altitude histories to orbit, Pegasus-type trajectory.

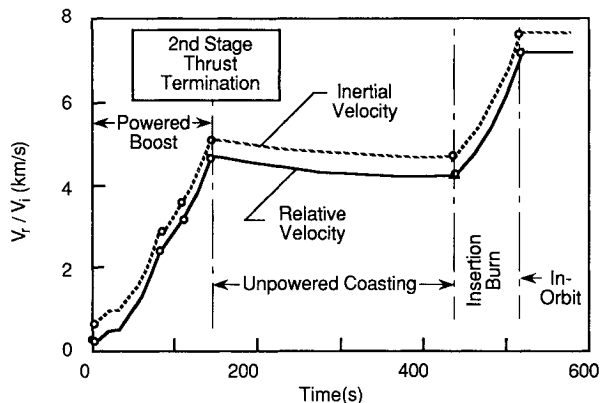


Fig. 14 Velocity histories to orbit, Pegasus-type trajectory.

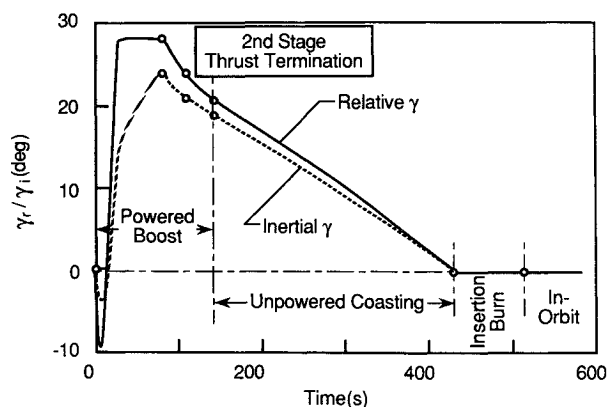


Fig. 15 Flight-path histories to orbit, Pegasus-type trajectory.

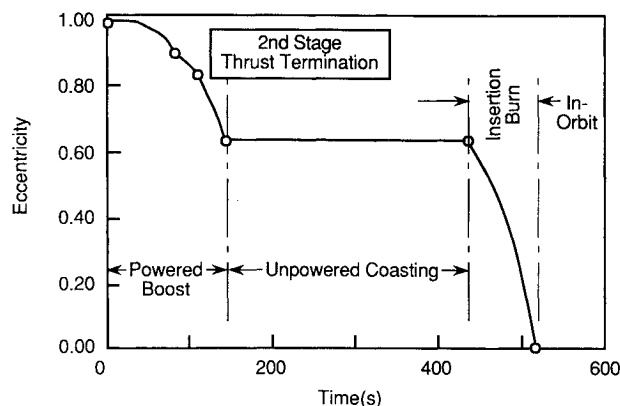


Fig. 16 Eccentricity history to orbit, Pegasus-type trajectory.

The altitude vs inertial velocity plot is shown in Fig. 12. The directions of flight are depicted with arrows. Below a 100-km altitude, nonlinear effects of aerodynamic deceleration that occurred during the unpowered descent and ascent phases are observed.

#### PEGASUS Flight Simulation

A sample trajectory of a PEGASUS flight<sup>9</sup> was simulated. The PEGASUS is a winged booster propelled by three solid rocket motor stages to place satellites into orbit. Because the propulsion performance is independent of atmospheric variation, an orbital condition will be satisfied by an exoatmospheric BO. The aerodynamic characteristics were estimated for a delta-wing/cylinder configuration. The rocket motor characteristics were approximated from Ref. 9. The trajectory simulation was initiated from the air-launched point ( $M = 0.8$ ,  $h = 12.2$  km) with a 5-s delayed ignition. During the first stage boost, a pull-up maneuver was programmed to follow along a steep climbing path ( $\gamma_r = 28$  deg), but the trajectory was not constrained on the dynamic pressure limit. The orbital altitude was arbitrarily targeted for a 365.7-km (1200-kft) circular orbit. The orbit transfer flight was taken along an equatorial orbit.

The apogee and actual altitude histories are shown in Fig. 13. The final second-stage powered boost was terminated in the exoatmosphere at 127 km altitude. The peak apogee achieved at the BO time was therefore almost equal to the targeted orbital altitude. As a consequence, essentially no aerodynamic drag penalty was imposed during the unpowered orbit transfer, as can be observed by a constant apogee climb.

The inertial and relative velocity histories are shown in Fig. 14. The event trapping procedure had properly captured the exoatmospheric BO condition. In this case the required inertial velocity at the thrust termination was defined only by Eq. (1), and no iteration of Eq. (3) was necessary. However, the

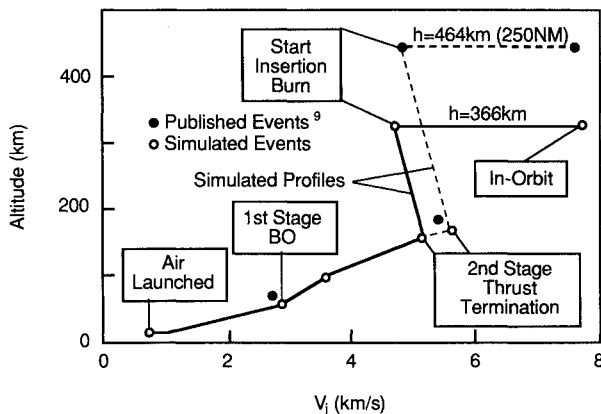


Fig. 17 Altitude vs inertial velocity, Pegasus-type trajectory.

BO inertial velocity of 5.134 km/s necessary to reach the orbit was considerably less than that for the previous case (7.93 km/s; see Fig. 4). This occurred because the steep power boost phase with the BO inertial flight-path angle of 18.7 deg (Fig. 15) had placed the final stage on a highly eccentric transfer ellipse ( $e = 0.6$ ; Fig. 16).

The energy deficiency for the orbit must be compensated during the orbital insertion burn as shown in Fig. 14. Because a finite time burn was executed, the thrust vector was modulated to maintain a zero flight-path angle to circularize the orbit. An eccentricity change from a highly eccentric transfer ellipse ( $e = 0.6$ ) to zero was achieved by the insertion burn as shown in Fig. 16.

The altitude vs inertial velocity plot is shown in Fig. 17. In this plot the simulated trajectory profiles for the orbital altitudes of 365.7 and 463.7 km (250 n.mi., given in Ref. 9) are included. The latter case was achieved by extending the second-stage burn time to attain the required orbital energy. The latter case is then compared with the published event data points<sup>9</sup> (solid circles). The discrepancies observed at the first- and second-stage thrust terminations were expected because the aerodynamic and propulsion estimates were not identical to the actual vehicle and the dynamic pressure constraint was not imposed in the present simulation. However, the in-orbit conditions were accurately simulated.

## Conclusions

An event trapping procedure was developed to define an endoatmospheric thrust-termination requirement for placing winged space vehicles into low Earth orbit. The technique was

based on application of a simple idea but is powerful enough to offer insight into the complex problem. In this ascent concept the required orbital transfer energy is dictated by a  $\Delta V$  loss produced during the endoatmospheric coasting event. Because this energy loss occurs as future events, the  $\Delta V$  estimation constitutes a highest degree of uncertainty. The success of orbital trajectory simulation therefore depends on the capability that captures a proper  $\Delta V$  loss during the boost phase.

The impact of a  $\Delta V$  penalty is equivalent to reaching a higher imaginary apogee that extends beyond the prescribed orbit. Sample cases have indicated that an imaginary apogee trace is a useful indicator for assessing the endo-/exoatmospheric thrust termination effects.

The derived event trapping procedure was incorporated in a point mass, three-dimensional trajectory simulation program.<sup>8</sup> Sample problems have demonstrated the ability of the technique to place a winged spacecraft precisely on a prescribed orbit. The methodology application is useful for investigating preliminary trajectories and conducting orbital transfer trade studies of winged spacecraft.

## References

- Small, W. J., Weidner, J. P., and Johnston, P. J., "SCRAMET Nozzle Design and Analysis as Applied to Highly Integrated Hypersonic Research Airplane," NASA TN D-8334, Nov. 1976.
- Ikawa, H., "Rapid Methodology for Design and Performance Prediction of Integrated Supersonic Combustion Ramjet Engine," *Journal of Propulsion and Power*, Vol. 7, No. 3, 1991, pp. 437-444.
- Brauer, G. L., Cornick, D. E., Olsen, D. W., Petersen, F. M., and Stevenson, R., "Program to Optimize Simulated Trajectory (POST): Volume II Utilization Manual," Martin Marietta, MCR-87-583, NAS1-18147, Denver, CO, Oct. 1986.
- Paris, S. W., and Hargraves, C. R., "Optimal Trajectories by Implicit Simulation (OTIS)," Boeing, AFWAL-TR-88-3057, Seattle, WA, Nov. 1988.
- Bate, R. R., Mueller, D. D., and White, J. E., *Fundamentals of Astrodynamics*, Dover, New York, 1971, pp. 11-49.
- Hoepfner, H., and Lampert, S., "Dimensionless Flight Mechanics: Part I—Space Flight in a Central Gravity Field," North American Aviation, SID 63-982, Downey, CA, revised March 1964.
- Ikawa, H., "Effect of Rotating Earth for Analysis of Aeroassisted Orbital Transfer Vehicles," *Journal of Guidance, Control, and Dynamics*, Vol. 11, No. 1, 1988, pp. 47-52.
- Ikawa, H., "A Unified Three-Dimensional Trajectory Simulation Methodology," *Journal of Guidance, Control, and Dynamics*, Vol. 9, No. 6, 1986, pp. 650-656.
- Covault, C., "Pegasus Winged Launch Vehicle: Commercial Winged Booster to Launch Satellites from B-52," *Aviation Week and Space Technology*, June 6, 1988, pp. 14-16.

James A. Martin  
Associate Editor